DOE/ET-53088-75 IFSR #75

KINETIC THEORY OF GLOBAL n=1 INSTABILITIES IN TOROIDAL PLASMAS

Kimitaka Itoh, Sanae-Inoue Itoh
Institute for Fusion Studies
The University of Texas at Austin
Austin, TX 78712
and
Takashi Tuda and Shinji Tokuda
Japan Atomic Energy Research Institute
Tokai, Ibaraki, 319-11, Japan

January 1983

Kinetic Theory of Global n=1 Instabilities in Toroidal Plasmas

Kimitaka Itoh*, Sanae-Inoue Itoh‡
Institute for Fusion Studies
The University of Texas at Austin
Austin, TX 78712

and

Takashi Tuda and Shinji Tokuda
Japan Atomic Energy Research Institute
Tokai, Ibaraki, 319-11, Japan

Permanent Address:

* Japan Atomic Energy Research Institute, Tokai, Ibaraki, 319-11, Japan

‡ Institute for Fusion Theory, Hiroshima University, Hiroshima, 730, JAPAN.

ABSTRACT

The kinetic theory of the global n=1 instabilities of finite-β tokamak plasmas with circular cross-sections is investigated in the collisionless limit. (n: toroidal mode number, β; plasma pressure normalized to the magnetic pressure). The wave-particle interactions and the finite gyroradius effect are included as kinetic corrections. The toroidal effect is incorporated up to the first order of $\varepsilon \equiv a/R$, the inverse aspect ratio. The radial-poloidal eigenmode equations are directly solved numerically in the parameter range $q(0) \sim 1$ (q: safety factor). Analytical studies of the modes are made by use of the energy integrals and compared to the numerical results. Special attentions are paid for studying the transition between the MHD-type mode and the kinetic instabilities.

The m=1 internal/tearing mode, n=1 ballooning mode and m=2 tearing mode with a fixed boundary condition are identified in connection with the MHD modes. When the q=1 mode-rational surface exists in the plasma, the m=1 internal mode has large growth rate in finite-β toroidal plasma; this mode turns out to be the m=1 collisionless tearing mode in the low β regime. The transition occurs around the parameters where the condition $\beta^2 \sim \varepsilon^2 \rho_i/a$ is satisfied (ρ_i/a: ion gyroradius divided by the plasma radius). The pressure driven ballooning mode, which becomes unstable when q-value becomes large and $\beta \gtrsim a/2q^2R$ in the MHD limit, is connected to the electrostatic-like ballooning mode which is unstable with the growth rate of the order of the drift frequency. The m=2 tearing mode is destabilized by the parallel current and is stabilized due to the

coupling with the drift branch when β-value increases. The toroidal coupling further stabilizes the m=2 tearing mode.

1. Introduction

Analyses based on the magnetohydrodynamic (MHD) theory have shown the existence of global unstable modes in tokamaks such as the kink mode, ballooning mode (pressure-driven mode) and tearing mode.[1-4] These modes are destabilized by either the plasma current or the pressure gradient (or both), and limit the stable region of operation to the low-pressure and low-current domain. As the plasma temperature increases, the kinetic interactions between plasma particles and waves are no longer negligibly small. The kinetic corrections on the MHD unstable mode has recently attracted attention[5-10] concerning the stability of the short-wave-length ballooning mode[11,12] which is also one candidate of the origin of the β-limit of toroidal plasmas (β is the ratio of the plasma pressure to the magnetic pressure). The kinetic effects have influences on the plasma stability in two ways: one is the change of the growth rate in the MHD unstable region, where the finite gyroradius effect is important. The other is the change of the stability criterion associated with the residual instability in the MHD stable region. These two effects are often competing and it has been shown that both the finite gyroradius effect and wave-particle resonance must be taken into account simultaneously. These effects are also important for the global mode stability. For example, the tearing mode stability is subject to a considerable change if one employs not the fluid resistivity but the kinetic parallel conductivity,[13-17] since the tearing mode is destabilized by the parallel resistivity near the rational surface. The previous work has indeed shown that the m=2 tearing mode turns to be a collisionless tearing mode[14,15] and is stabilized by ion Landau damping in high temperature and high-β

plasmas.[16,17] However the work has been restricted to the cylindrical plasma, and no clear understandings have been obtained in the toroidal geometry, where the two instability origins - plasma current and toroidal curvature - coexist simultaneously.

In this paper we investigate the stability of the n=1 mode (n: toroidal mode number) in a circular-cross-sectional tokamak with small but finite β values ($\beta_p \sim 1$; β_p being the plasma pressure normalized to the poloidal magnetic energy), by employing the kinetic analyses. The study is performed in the large-aspect-ratio limit of the collisionless high temperature plasmas, and the stability of incompressible mode (i.e. the toroidal magnetic field perturbation is neglected) is investigated. In order to study the kinetic effects near the marginal stability condition of the MHD mode and the toroidal effects on the intrinsic kinetic instability, we take the ∇B and curvature drift of particles into account and keep the lowest order toroidal corrections. Our model satisfies the criterion that it recovers the stability condition of the reduced-set MHD analyses in the MHD limit where $\tilde{E}_{\parallel} \to 0$ and the gyroradius is neglected.

The radial-poloidal eigenmode is obtained with the fixed boundary conditions. The "m=1" internal[18-20] and tearing modes,[21-22] n=1 (pressure-driven) ballooning mode and "m=2" tearing mode are identified. The stability region is investigated and attentions are paid to the transition near the MHD stability criteria. The "m=1" internal mode, which is unstable in the finite-β toroidal plasma if the q=1 rational surface exists in the plasma column, turns to be the "m=1" collisionless tearing mode in the low-β region. Other strong instability is the ballooning mode which has the critical β value

($\beta_c \sim a/2q^2R$) in the MHD theory. This mode is connected to the electrostatic-like ballooning mode (associated with the ion drift mode) which persists to be unstable in the low-β limit. The "m=2" tearing mode is stabilized due to the coupling with the drift mode if the β-value increases. The toroidal effect further stabilizes the m=2 tearing mode. Contrary to the high-n modes,[9] the mode coupling does not prohibit the radial convective damping of the m=2 tearing mode, since the distance between q=2 and q=1 surfaces is much larger than the ion-Landau-damping length, $|\omega/k_\parallel' v_i|$. The toroidal coupling allows the energy flow from m=2 mode to the m=1 mode, and this energy flow acts as an additional damping mechanism of the m=2 tearing mode.

The constitution of this paper is as follows: In Section 2 the model and the basic equation are given. In Section 3 the eigenmodes and eigenvalues for n=1 modes are obtained. Summary and discussion are given in the final section. The trapped particles contribute principally to the dissipation and the poloidal coupling is not enhanced much by the existence of trapped electrons. We therefore neglect the trapped particle contributions for simplicity and the analytical insight.

2. Model and Basic Equation

We take the plasma equilibrium with circular magnetic surfaces. Due to the toroidal shift of the magnetic axis, the geometrical axis of the magnetic surface of the radius r deviates from the major axis of the torus by the quantity $\Delta(r)$. The Figure 1 shows the schematic geometry of the equilibrium. The coordinates (r,θ,ζ), where r,θ and ζ are the minor radius, poloidal angle and toroidal angle, are given by the cylindrical coordinates (R,ζ,z) as $R = R_0 + \Delta + r\cos\theta$ and $z = r\sin\theta$. We use the coordinates (r,η,ζ) which represent the magnetic field line to be "straight", defining

$$\theta = \eta + \Lambda \sin\eta \tag{1}$$

and $\Lambda \equiv -\Delta' + r/R$. The poloidal magnetic field is given by $B_\theta = \bar{B}_\theta(r)(1-\Delta'\cos\theta)$. The metric tensor g_{ij} is calculated to be

$$g_{11} = (1 + \Delta'\cos\eta)^2 + (\Delta' - r\Lambda')^2\sin^2\eta \ , \tag{2-1}$$

$$g_{12} = r(-\Delta' + r\Lambda')(1 + \Lambda\cos\eta)\sin\eta \ , \tag{2-2}$$

$$g_{22} = r^2(1 + \Lambda\cos\eta)^2 \tag{2-3}$$

$$g_{33} = R_0^2\{1 + (r/R_0)\cos\eta\}^2 \ . \tag{2-4}$$

Due to the toroidal shift of the axis, g_{12} remains finite and the coordinates are not orthogonal. The safety factor is given by the derivative along the field line as

$$q(r) = d\zeta/d\eta \ . \tag{3}$$

Since we treat the cases of the moderate β_p where $\beta_p \sim O(1)$ holds (β_p is the poloidal β-value), we keep the first order terms of the toroidal corrections. The Jacobian of the transformation is approximated to be $\sqrt{G} \simeq R_0 r\{1+(2r/R_0)\cos\eta\}$. The equilibrium magnetic field and pressure profile must be determined by the toroidal equilibrium equation. Expanding the pressure profile with respect to the inverse aspect ratio, r/R_0, and keeping the first order terms, the toroidal equilibrium is given by the corresponding cylindrical distribution as[23]

$$\psi = \psi_0(r) + \psi_1(r)\cos\Theta \ , \tag{4}$$

$$\psi_1(r) = \frac{d\psi_0}{dr}\left[\int_a^r dr' \frac{1}{r'(d\psi_0/dr')^2}\int_0^{r'}\left\{\frac{r''}{R}\left(\frac{d\psi_0}{dr''}\right)^2 - 2\mu_0 R r''^2 \frac{dp_0}{dr''}\right\}\right] \tag{4-2}$$

where $\psi(r,\Theta)$ is the poloidal magnetic flux function. Therefore, up to the first order corrections of a/R_0, the MHD equilibrium can be specified by $p_0(r)$ and $q(r)$ (or $J_0(r)$). The toroidal shift of the magnetic surface Δ is given as

$$\Delta = \int_r^0 dr' \frac{1}{r'(d\psi_0/dr')^2}\int_0^{r'}\left\{\frac{r''}{R}\left(\frac{d\psi_0}{dr''}\right)^2 - 2\mu_0 r''^2 \frac{dp_0}{dr''}\right\} \ . \tag{5}$$

We introduce the Fourier decomposed representation for fluctuations, e.g.,

$$\tilde{B}_r(\vec{r},t) = \sum_m B_{rm}(r)\exp(im\eta - in\zeta - i\omega t) \ .$$

Owing to the axial symmetry, each toroidal component can be treated separately and the suffix for n is suppressed.

The equilibrium distribution function is chosen to be shifted local Maxwellian. The density N is inhomogeneous (and is a function of the poloidal angular momentum P_ζ). The temperature is assumed to be constant to satisfy that the plasma is collisionless in the whole plasma column. The pressure gradient is, in this article, due to the density gradient.

The linearized equations for the Vlasov-Maxwell system are solved to get the perturbation distribution function $\tilde{f}$. The quasi-neutrality condition and the Ampere's law yield the basic equation for $\tilde{E}_\eta$ and $\tilde{B}_r$. The coupled differential equation is derived,[24]

$$a^2(\nabla_\perp^2\phi)_m - \frac{\Omega}{\tau\Omega+m}\Big[P_m(\phi_m + \zeta_m\psi_m)$$

$$+ \frac{\varepsilon}{\Omega}\Big\{\frac{m(1+\tau)}{\tau\Omega}\frac{a^2}{p_i^2} + R_m\Big\}\Big[\Big\{(m-1) - x\frac{\partial}{\partial x}\Big\}\phi_{m-1} + \Big\{(m+1) + x\frac{\partial}{\partial x}\Big\}\phi_{m+1}\Big]\Big] = 0 \quad (6\text{-}1)$$

$$a^2(\nabla^2\psi)_m - \frac{m\beta_i\sqrt{2}u}{\Omega c_s}\frac{a^2}{\rho_i^2}\psi_m + 2\beta\zeta_m\left[P_m(\phi_m+\zeta_m)\right.$$

$$\left. + \frac{\varepsilon R_m}{\Omega}\left[\left\{(m-1) - x\frac{\partial}{\partial x}\right\}\phi_{m-1} + \left\{(m+1) + x\frac{\partial}{\partial x}\right\}\phi_{m+1}\right]\right] = 0 \quad m \geq 1 \qquad (6\text{-}2)$$

where $\phi_m = x\tilde{E}_{\eta m}$, $\psi_m = \sqrt{2}v_i x\tilde{B}_{rm}/c$, $x = r/a$, a is the plasma radius, $\Omega = \omega(2scT_e/a^2eB)^{-1}$, $N_0(r) = N(0)\exp(-sr^2/a^2)$, $\zeta_m = \omega/\sqrt{2}k_\parallel^{(m)}v_i$, $k_\parallel^{(m)} = (m/q-n)/R$, $v_j^2 = T_j/M_j$ (j = i or e), $\varepsilon = L_n/R$, $\tau = T_e/T_i$, ρ_i is the ion gyroradius, $u = -J_0/N_0e$, $\beta_i = 4\pi N_0T_i/B^2$, $c_s^2 = T_e/M_i$, $\beta = 2(1+\tau)\beta_i$,

$$P_m = \frac{a^2}{\rho_i^2}\left[\frac{m-\Omega}{2\Omega}Z'(\xi_{em}) - \frac{\Omega\tau+m}{\Omega}Z'(\xi_{im}) - \frac{k_\parallel^{(m)}u}{\sqrt{2}|k_\parallel^{(m)}|v_e}\left\{Z(\xi_{em}) + \frac{\Omega-m}{\Omega}\xi_{em}Z'(\xi_{em})\right\}\right],$$

$$R_m = \frac{a^2}{\rho_i^2}\left[\frac{m-\Omega}{2\Omega}\left\{Z'(\xi_{em}) - \frac{\xi_{em}}{2}Z''(\xi_{em})\right\} + \frac{\Omega\tau+m}{2\Omega\tau}\left\{Z'(\xi_{im}) - \frac{\xi_{im}}{2}Z''(\xi_{im})\right\}\right],$$

Z is the plasma dispersion function of the argument $\xi_{jm} = \omega/\sqrt{2}|k_\parallel^{(m)}|v_j$. In deriving Eq. (16), we use the ordering for the kinetic corrections, i.e., such as $\rho_i^2\nabla_\perp^2$, $\tilde{E}_\parallel$, β and u/v_e are of the first order smallness. Another simplification is the expansion with respect to ε. By taking the toroidal drift of particles, we retain the driving source of the toroidal MHD mode. The MHD limit of Eq. (6) is equivalent to the reduced set equations. Since we are interested in the small β_i plasma, we neglect the compressional component of the magnetic field perturbation $\tilde{B}_\zeta$ and the m=0 component of the

perturbations. By Eq. (6), one can study the transition between MHD mode and kinetic mode as well as see the toroidal effect on the intrinsic kinetic mode in the medium β_p regime.

The equation (6) is a set of coupled equations, and in principle, all m components can contribute to the eigenmode. However, we can truncate the m-summation at a certain value of m for n=1 mode by the following reasons. When m is far from the q value of the column, the m-component is successively induced through toroidal coupling and is of the higher order of r/R_0: such component is to be neglected due to the ordering of ε. We study the n=1 fixed-boundary mode in the low-q regime, i.e., $q(0) \sim 1$, and the main Fourier component is m=1 and 2. We truncate the m-summation at m=3 or 4. The truncation is also found, a posteriori, to be a good approximation.

3. Stability Analysis

We solve Eq. (6) for n=1 modes with the fixed boundary condition and find the "m=1" internal/tearing mode, the "m=2" tearing mode and the n=1 ballooning mode. To solve the perspective view about the various modes, we illustrate the stability diagram in q-β plane in Figure 2. The temperature of the plasma is taken into account through the parameter ρ_i/a. As the equilibrium we chose the Gaussian profile for density and current as $n_0(r) = n_0\exp(-sx^2)$ and $J_0(r) = J_0\exp(-sx^2)$. The q profile is given as

$$q(r) = q(0)\frac{sx^2}{1-\exp(-sx^2)}, \tag{7}$$

and the average β-value, $\langle\beta\rangle$, is given as $\langle\beta\rangle = \beta(0)(1-e^{-s})/s$. We choose the parameter such as a/R = 0.25 and s = 2.25. q(a)/q(0) = 2.52 holds. For kinetic parameters, we choose $\rho_i/a = 1/200$, $M_i/M_e = 1836$ and $T_i = T_e$. The "m=1" instability appears when the mode rational surface r_1, q(r) = 1, exists in the plasma column, and the transition between internal and tearing modes is found. When β_p becomes large, the ballooning mode becomes unstable by the MHD mechanism, but turns to be electrostatic-like ballooning instability[25] in the low-β_p region. The importance is the stability of the "m=2" tearing mode in the finite-β region, which was not explored in the MHD analyses. The figure shows that there always exists instability for any plasma parameters. Therefore, analyses are focused to know their growth rates, etc. In the following subsections we study, one by one, the stability condition, parameter dependence and the mode structure.

3-1. "m=1" Mode

The "m=1" mode is destabilized by two mechanisms. One is the pressure gradient of the plasma, and the MHD theory[18] predicts the instability with the growth rate which is typically scaled as β_p^2. Secondly, the wave-particle interactions near the mode rational surface causes the residual kinetic instability, when the plasma β value decreases while the q-value and other parameters are fixed. In this case, the electron drift which carries the parallel current, u, becomes large. The transition between the MHD mode and the kinetic mode is found. This transition is important to understand the β-dependence of the m=1 mode stability and consequently the internal disruption problem.

The m=1 Fourier component is dominant for this mode. The amplitude of the m=3 component is $O(\varepsilon^2)$ and gives a small correction. We truncate the m-summation up to m=2 or m=3 and compare the results. We have confirmed that the coupling between m=1 and 2 modes is essential. Therefore we calculate the energy integral keeping the m=1 and m=2 components to obtain the analytical understandings, i.e.,

$$\sum_{m=1}^{2}(k_m+W_m) + W_{12} = \sum_{m=1}^{2}\frac{\omega^2}{\tau}\int_0^1 \frac{c^2}{\rho_i^2 V_A^2} P_m|\phi_m + \frac{\omega}{k_\parallel^{(m)} c}\psi_m|^2 x dx \qquad (8)$$

where

$$K_m = \omega\left(\omega + \frac{\omega_*}{\tau}\right) \int_0^1 x dx \frac{c^2}{V_A^2} \{ |\phi_m'|^2 + k^2 |\phi_m|^2 \}$$

$$W_m = -|\omega|^2 \int_0^1 x dx \{ |\psi_m'|^2 + \left(k^2 + \frac{4\pi}{c} \frac{kJ_0'}{k_\parallel^{(m)} B_0}\right) |\psi_m|^2 \}$$

$$W_{12} = \int_0^1 x dx \, 8\varepsilon \frac{c^2}{a^2} \beta(0) s^2 \{ \phi_1^* (2 + x \frac{\partial}{\partial x}) \phi_2 + 2\phi_2^* (1 - x \frac{\partial}{\partial x}) \phi_1 \} ,$$

$\omega_A = V_A/R_0$, $V_A = B_0/\sqrt{4\pi N_0 M_i}$, $\omega_* = 2msT_e c/eBa^2$. Terms K_m, W_m and W_{12} in the left-hand side correspond to the kinetic energy of the perpendicular motion, the restoring magnetic energy and the one due to bad curvature and the ballooning of displacement through toroidal couplings, respectively. The right-hand side is due to the dissipation via wave-particle interaction through parallel electric field.

Let us evaluate each term for this mode. The MHD theory predicts that the amplitude of ϕ_1 vanishes outside of the mode rational surface, $q > 1$, for the most unstable mode.[18] Its eigenmode structure has sharp gradient near the mode rational surface. When the parallel phase velocity is much smaller than the Alfvén velocity, $V_A^2 >> |\omega/k_\parallel^{(1)}|^2$, the Alfvén potential associated with the bending of the field line dominates; MHD mode is most unstable with the radial displacement ξ_{r1}, $\xi_{r1} \sim \phi_1/x$, which satisfies the condition $d\xi_{r1}/dx \sim 0$ for $q < 1$.[18] On the contrary, in the vicinity of the rational surface, $k_\parallel^{(1)}$ goes to zero and the condition

$$|k_\parallel^{(1)} V_A|^2 \lesssim |\omega|^2 \qquad (9)$$

is satisfied across the surface $x_1 - \delta < x < x_1 + \delta$. In this region, the kinetic effect becomes noticeable. We estimate δ, to be

$$\delta \sim \frac{|\omega|}{a|dk_{\parallel}^{(1)}/dr|V_A} , \tag{10}$$

and divide the plasma column to obtain the approximate solution. The most unstable mode is realized for $W_1, W_2 \sim 0$. Noting the condition of ξ_{r1}, we choose

$$\phi_1 \sim \begin{cases} \hat{\phi} x & 0 \leqslant x < x_1-\delta \\ \hat{\phi} \dfrac{(x_1-\delta)}{2\delta}(x_1+\delta-x) & x_1-\delta \leqslant x \leqslant x_1+\delta \\ 0 & x_1+\delta \leqslant x \leqslant 1 . \end{cases} \tag{11-1}$$

ϕ_2 is then given as

$$\phi_2 \sim \begin{cases} \varepsilon\beta_p \hat{\phi}\, x^2 & 0 \leqslant x < x_1-\delta \\ \varepsilon\beta_p \hat{\phi}\, x_1^2 & x_1-\delta \leqslant x \leqslant x_1+\delta . \end{cases} \tag{11-2}$$

The derivative ϕ_1' becomes large for $x_1-\delta < x < x_1+\delta$ and is approximated to be $-\hat{\phi}/2\delta$. Hence W_{12} is evaluated to be

$$W_{12} \sim 12\varepsilon^2\beta_p\beta(0)s^2\,\hat{\phi}^2\,\frac{c^2}{a^2} \tag{12}$$

and the kinetic energy is approximately given as

$$K_1 \sim \frac{\omega(\omega+\omega_*)}{2\delta}\hat{\phi}^2\frac{c^2}{V_A^2} . \tag{13}$$

The parallel electric field exists in the vicinity of the rational surface, $|x-x_1| \leqslant \delta$, and the integrand in the right-hand side of Eq. (8) is non-vanishing for $|x-x_1| \lesssim \delta$. Since we treat the wave-particle interaction to be the first-order smallness, we evaluate $E_{\parallel 1}$ in the cylindrical limit. The equation (6-1) gives

$$\phi_1 + \frac{\omega\psi_1}{k_\parallel^{(1)}c} \sim -\frac{\omega+\omega_*}{P\omega}\frac{\phi_1}{\delta^2} . \tag{14}$$

Substituting this relation into the integral of Eq. (8), we have

$$\omega^2 \int_0^1 \frac{c^2}{\rho_i^2 V_A^2} P_1 \left|\phi_1 + \frac{\omega\psi_1}{k_\parallel^{(1)}c}\right|^2 xdx \sim x_1 \frac{c^2}{V_A^2}(\omega+\omega_*)^2 \frac{1}{\langle P_1\rangle}\frac{\hat{\phi}^2}{\delta^3 a} \tag{15}$$

where $\langle P_1\rangle$ is the average of P_1. The $\nabla p \times \nabla B$ driving force, kinetic energy and dissipation by wave-particle interaction balances to give

$$\frac{\omega(\omega+\omega_*)}{2\delta} + 12\,\beta_p\beta(0)s^2\omega_A^2 = (\omega+\omega_*)^2\frac{x_1}{\langle P_1\rangle}\frac{1}{\delta^3 a} . \tag{16}$$

The first term includes the finite gyroradius stabilization effect[5,16]

and the right-hand side gives the dissipation and residual/intrinsic kinetic instabilities; two essential kinetic corrections are included.

The dispersion relation (16) gives two kinds of instabilities and the transition between them. Two limiting cases are solved as

$$\frac{\gamma}{\omega_A} \sim \begin{cases} \varepsilon^2\beta_p^2 \dfrac{1}{aR|k_\parallel^{(1)}|'q^2} & \text{MHD-limit} \quad (17\text{-}1) \\ \left[8s^2s^2k_\parallel^{(1)}x_1\right]^{1/3}\beta_i^{1/3}\dfrac{\rho_i}{a} & \text{kinetic-limit} \quad (17\text{-}2) \end{cases}$$

where we use $\langle P_1\rangle \sim (\omega_*-\omega)\langle 1+\xi_e Z\rangle/\omega$ and evaluated the average of $\xi_e\exp(-\xi_e^2)$ to be of the order of unity. The MHD growth rate gives $\gamma/\omega_A \propto \varepsilon^2\beta_p^2$ while the kinetic growth rate shows a weaker dependence on ε or β.* The mode becomes MHD-like for higher β-values, while it turns out to be the kinetic mode in the low-β region. The transition occurs for $\gamma_{MHD} \sim \gamma_{kinetic}$: the result in Figure 2 is understood from Eq. (17).

Numerical calculation is performed for the "m=1" mode, keeping m=1,2 and 3 components.

The Figure 3 shows the growth rate of the "m=1" toroidal mode as a function of β_p. We choose the parameter $\rho_i/a = 1/200$, $q_0 = 0.9$, $s = 2.25$, $R/a = 4$, $T_e/T_i = 2$ and $M_i/M_e = 1836$. The dashed line is for the MHD limit approximation, where we take $\tilde{E}_\parallel = 0$ and $\rho_i/a = 0$, which shows $\gamma/\omega_A(MHD) \propto \beta_p^2$ confirming Eq. (17-1). The solid line is the

---

* If one decreaes β_i by reducing the density, the electron parallel velocity increases and the current-driven term dominates in $\mathrm{Im}\langle P\rangle$, and γ/ω_A deviates from Eq. (17).

growth rate in the presence of the kinetic interactions. For larger β_p, $\gamma \propto \beta_p^2$ holds, while the deviation becomes large for small β values. The mode turns to be the residual instability caused by the Landau resonance. The contribution of the resonance is proportional to ρ_i/a as estimated in Eq. (17-2). The Figure 4 shows the ρ_i/a dependence of the growth rate for various values of β_i. The growth rate linearly increases as ρ_i/a increases, conforming Eq. (17-2). The a/R dependence of γ, Figure 5 shows the toroidally induced MHD mode and the kinetic instability in the $a/R \to 0$ limit. The q-dependence of γ more clearly shows the transition between the kinetic mode and the MHD mode in Figure 6. Also shown are the MHD limit (dotted line) - we call it MHD internal-like - and the cylindrical kinetic limit - that is the m=1 collisionless tearing mode where the ∇B drift is neglected (dashed line). As q increases, β_p increases for fixed β-values accordingly the connection length becomes larger, and $dk_\parallel^{(1)}/dx$ decreases at the same time. The MHD type driving force dominates the instability mechanism. On the other hand, as $q(0)$ becomes small, q is reduced and the mode rational surface approaches the edge. Accordingly, $x_1 k_\parallel^{(1)\prime}$ increases and the cylindrical m=1 kinetic mode is strongly destabilized.

The mode structures are shown in Figures 7a and 7b for the MHD-like internal mode and m=1 tearing mode. The Figure 7a is for $\beta_i = 1/200$ and $q(0) = 0.9$, where the m=1 internal mode is destabilized by the MHD mechanism. The m=1 component is found inside the q=1 surface and the m=2 component is also confined inside of the q=2 surface. $\phi_1 = xE_{\eta 1}$ shows a sharp decrease at $r = r_1$, confirming Eq. (11). The corrugation near the rational surface shows

the coupling with the drift branch. The lower column is for the parallel electric field which becomes large in the vicinity of the rational surface. The Figure 7b is for the "m=1" tearing mode, which is found in the low q_0 case, $q_0 = 0.4$. One sees that B_{r1} is non-zero at $r=r_1$ and the mode has the character of the tearing mode with localized parallel electric field and is not subject to the radial convective damping. The exudation of the B_{r1} across the q=1 rational surface is, however, much smaller than the case of the simple resistivity driven m=1 mode.[21] The associated reconnection may become much more moderate in high temperature plasmas.

3-2 Ballooning Mode

When q-value becomes high and q(0) is greater than unity, the m=1 internal mode disappears and the most unstable mode is characterized by the dominant m=2 component. The MHD instability ballooning mode and tearing instability are possible in finite-β toroidal plasma; these two modes are different branches from the view point of the eigenmode structures.

We first study the ballooning mode. This mode is characterized as an MHD type instability driven by the $\nabla p \nabla B$ force if β-value is high and exeeds a critical value. The terms in the energy integral is also derived for the test function

$$\phi_2 \sim \begin{cases} \hat{\phi} x^2 & x < x_2-\delta \\ \dfrac{\hat{\phi}}{2\delta}(x_2-\delta)^2(x_2+\delta-x) & x_2-\delta < x < x_2+\delta \\ 0 & x_2+\delta < x < 1 \end{cases} \qquad (18)$$

where we consider the case $q(0) < 2 < q(a)$ and $q(x_2) = 2$ holds. In this case $m=2$ component is the dominant term and $m=1$ and 3 component are excited by toroidal coupling and is estimated to be

$$\begin{pmatrix} \phi_1 \\ \\ \phi_3 \end{pmatrix} \sim \begin{pmatrix} \varepsilon\beta_p\hat{\phi}x \\ \\ \varepsilon\beta_p\hat{\phi}x^3 \end{pmatrix} \qquad 0 < x < x_2 \ . \tag{19}$$

The fluid motion is also localized in the vicinity of the $q=2$ mode rational surface, similar to the $m=1$ case. The kinetic energy K_2 can be estimated to be $K_2 \sim \omega(\omega+\omega_*)c^2\hat{\phi}^2/2\delta V_A^2$. For $m=2$ mode, the magnetic restoring energy, W_2, has a stabilization influence of the order of

$$W_2 \simeq - c^2\hat{\phi}^2 a^2 |k_\parallel'|^2 \ . \tag{20}$$

Hence the energy integral for the ballooning mode is given as

$$\frac{\omega(\omega+\omega_*)}{2\delta} + 24\,\beta_p\beta(0)s^2\omega_A^2 - \omega_A^2a^2R^2|k_\parallel'|^2 = (\omega+\omega_*)^2\,\frac{x_2}{\langle P_2\rangle}\,\frac{1}{\delta^3 a} \tag{21}$$

with the condition $\delta \sim |\omega|/a|k_\parallel^{(2)\prime}|V_A$. This equation shows the balance between the inertia term, ballooning destabilization term, Alfvén potential which is stabilizing and the wave-particle interaction contribution. Note that, in Eq. (21), ω_* is defined by $m=2$ and terms such as δ, ω_*, ω_A, $|k_\parallel'|$ and ρ_i are evaluated by the plasma parameter at $r=r_2$.

When the kinetic correction is weak, the MHD instability appears if the condition

$$\beta_p > \beta_{pc} \sim \frac{1}{\sqrt{6}} \left|\frac{aq'}{q}\right| \frac{R}{a} \tag{22}$$

holds. The critical poloidal beta value β_{pc} is given in the form $\beta_{pc} \sim C\ R/a$, where the numerical coefficient C is approximated to be $1/3$ or $1/2$ and has a weak dependence on the q value. On the contrary, the kinetic instability with the growth rate of the order of ω_* is possible if the condition Eq. (22) is not satisfied.

The β-dependence of the growth rate is shown in Figure 8 for the parameters of $q_0 = 1.7$, $s = 2.25$, $a/R = 1/3$, $\rho_i/a = 1/200$ and $T_e/T_i = 2$. The mode is found to be always unstable, showing the transition near the critical β value of the MHD stability. The dashed line is the growth rate derived by the MHD approximation ($\rho_i/a \to 0$, $\tilde{E}_\parallel \to 0$), and the dotted line denotes γ/ω_* which shows that the growth rate of the residual instability is proportional to ω_*. The residual mode, which is connected to the electrostatic branch in the zero-β limit, has the growth rate proportional to $\sqrt{\beta}$, so that the β-dependence is fairly weak; the growth rate can be comparable to the MHD limit in the region $\beta_p < \beta_{pc}$. The MHD destabilization force is governed by β_p, and the transition is observed by changing q while other parameters such as β are fixed. The kinetic effect is more clearly seen by studying ρ_i/a dependence of the eigenvalue. The Figure 9 shows ω/ω_A and γ/ω_A for the MHD unstable parameter $q_0 = 1.7$ (solid lines) for the parameters $\beta_i = 1/200$, $R/a = 3$ and $s = 2.25$. For the MHD unstable case the noticeable is that the real frequency

downshift appears. This is understood as follows; when one neglects the wave particle interaction, i.e., the right-hand side of Eq. (21), ω is given as

$$\omega \simeq -\frac{\omega_*}{\tau} + i\gamma_{MHD} \tag{23}$$

assuming that $\gamma_{MHD} >> \omega_*$ (γ_{MHD} is the growth rate in the MHD limit). This is because the kinetic energy of the fluid motion is proportional to $\omega(\omega+\omega_*)$ not to ω^2; therefore the stability condition for the reactive mode is relaxed as

$$\gamma_{MHD} > \frac{1}{2\tau}\omega_* \tag{24}$$

not $\gamma_{MHD} > 0$. This result is known as the finite gyroradius stabilization of the MHD mode.[5,26] However, the wave-particle interaction has the contribution of the same order of ρ_i/a as compared to the simple ω_* correction. The destabilization by the Landau damping cancels this stabilization and $\partial\gamma/\partial(\rho_i/a) \to 0$ in the zero-ρ_i/a limit. For this kind of global mode the destabilization by the wave-particle interaction results in a weak increase of γ as ρ_i/a increases, if the ion Landau damping is not effective. On the contrary to the MHD unstable case, the instability is purely kinetic driven in the parameter range $\beta_p < \beta_{pc}$. In Figure 9, also shown is the γ/ω_A value for the MHD stable parameter, $q_0 = 1.2$, (by dashed line) which is positive only if ρ_i/a is finite. Thus the mode connects to the branch of the electrostatic ballooning mode.

The mode structures are shown in Figure 10 and these two cases are compared. The Figure 10(a) is for the MHD unstable case. The m=2 component is the main component, and the peak of $\tilde{E}_{\theta 2}$ near the η=2 surface is broad since the growth rate is large. Typical to the MHD-like mode, the m=2 component of the parallel electric field has very small amplitude near the q=2 surface r_2. The parameters are $q_0 = 1.7$, $\beta_i = 1/200$, $R/a = 3$, $s = 2.25$ and other parameters are standard. By reducing β-value, this mode reduces to a kinetic mode. It is noted that for this n=1 ballooning mode the radial magnetic field perturbation vanishes on the rational surface as is shown in Figure 10(a). For instance, B_{r2} changes sign across the surface r_2. This mode is twisting mode like and is not connected to the "m=2" tearing mode. The Figure 10(b) is for $\beta_i = 1/1000$. The electric component E_θ shows a strong peaking near the q=2 surface, but has still a finite width due to the ω_* effect. It should be noted that the m=2 parallel electric field component peaks near q=2 rational surface.

3-3 "m=2" Tearing Mode

The "m=2" kinetic tearing mode is also identified in the toroidal plasma. This mode is characterized by the radial magnetic field perturbation which does not vanish at the mode rational surface. Also the parallel current at the rational surface plays an essential role for stability. This mode propagates in the electron diamagnetic drift and belongs to the shear-Alfvén branch of the plasma oscillations.[27,28] The Figure 11 shows the eigenmode structure of the "m=2" tearing mode for the parameters $q_0 = 0.9$, $\beta_i = 0.001$, s=3, $R/a = 3$ and other parameters are standard. The eigenvalue is given

$\omega/\omega_* \simeq 1+0.02i$. The parallel electric field clearly shows the coupling to the drift mode associated with the out-going energy propagation. The energy is absorbed by ions through Landau damping.[15-17] This is the important mechanism to dictate the stability. In addition to it the coupling to m=1 mode also acts as an additional damping. The distance between mode rational surfaces, $|r_2-r_1|$, is larger compared to the ion-Landau-damping-length, $|\omega_*/v_i k_\parallel'|$. Therefore, the coupling to the m=1 mode does not prohibit the convective damping but acts as an additional sink for the m=2 mode energy.* The stabilization by the finite-β effect is first found in the cylindrical geometry.[16] This stability improvement in higher-β regime persists in toroidal plasmas. The Figure 12 shows the growth rate as a function of β_i. The cylindrical case is also shown by the dashed line. The critical stability condition is studied and illustrated in Figure 13 and we find the condition

$$\beta > \beta_c \qquad (25\text{-}1)$$

for stability and

$$\beta_c \propto \rho_i/a \ . \qquad (25\text{-}2)$$

* The case is contrary for high-n modes, where distance between two successive mode rational surfaces, $1/|nq'|$, is much shorter than the ion Landau damping length. The stabilization by the toroidal effect is also observed for electromagnetic drift mode.

The Equation (25) shows that the critical condition for the stability is determined by the kinetic process, analogous to the cylindrical calculations.[16] From Eq. (18), one sees that the marginal stability condition is given by

$$\mathrm{Im} \sum_m \int_0^1 \frac{c^2}{\rho_i^2 V_A^2} P_m \left| \phi_m + \frac{\omega}{k_\parallel^{(m)} c} \psi_m \right|^2 x dx = 0 \tag{26}$$

which means that the excitation by electrons and convective damping balances. This condition is essentially the same as the drift and drift-Alfvén wave stability if one applies Eq. (26) for short wave length modes. As is shown by Eq. (15), the resonance contribution, Eq. (26), is of the order of $|\omega_*/(\omega-\omega_*)| \times \rho_i^2/a^2$. Therefore, for the modes which have the real frequency $\omega \sim \omega_*$ (such as drift mode or m=2 tearing mode), the resonance term, Eq. (26), has the leading contribution in Eq. (21). The stability condition, in the first approximation, is given as[28] ($\varepsilon \to 0$)

$$\frac{u}{v_i} \gtrsim C \sqrt{\frac{M_i}{M_c}} \frac{L_n}{L_s} \tag{27}$$

where L_n and L_s are the density gradient scale and the shear length respectively. C is the numerical coefficient of the order of unity. The parallel current have upper limit for stability. Recalling the relation

$$\frac{u}{v_i} = \frac{2}{q_0}\frac{a}{R}\frac{1}{\beta_0}\frac{\rho_i}{a} \tag{28}$$

and $L_n/L_s \sim a^2q'/2mRq^2$, Eq. (27) gives an evaluation at the q=2 mode rational surface as

$$\beta_i \gtrsim \frac{1}{Caq'q_0}\frac{\rho_i}{a} \tag{29}$$

stability. The coefficient $1/Caq'(r_2)q_0$ is of the order of unity, and Eq. (29) confirms the result of Figure 13. The stability diagram on the $q_0 - \beta_i$ plane is given by Figure 14 for the parameters $\rho_i/a = 1/200$, $R/a = 3$, $s=3$, and other parameters are standard. Comparing to the cylindrical limit, the critical β-value as well as the critical current density are reduced by the factor 2 due to the toroidal coupling. The Figure 15 shows the eigenmode structure for the stable "m=2" tearing mode where β_i is taken to be 0.01. The coupling to the m=1 mode is noticeable. The eigenvalue is given as $\omega/\omega_* \simeq 1 - 0.05i$.

4. Summary and Discussion

In summary, we have studied kinetic efects on n=1 global modes of the large aspect ratio tokamak in the collisionless limit. By solving the kinetic equation, the "m=1" internal/tearing mode, ballooning mode and "m=2" tearing mode are identified. The MHD driving term and the kinetic interactions are simultaneously included, and the transition between the MHD mode and the residual kinetic mode are found near the critical condition of the MHD instability. The toroidal effect on the collisionless tearing mode is found to be stabilizing. The stability of the m=2 tearing mode in the high-β region is still expected in the toroidal geometry. The eigenmodes are obtained by use of the fixed boundary conditions. As a result of this condition, m=2 kink mode becomes stabilized. In the case of a free boundary condition, the growth rate and the critical β-value for "m=2" tearing mode may increase. The marginal stability condition is still determined by Eq. (26), and the stability at high-β plasma holds.

The high temperature phenomena appear as finite-gyroradius-effect and wave-particle interaction. These two effects on the unstable MHD mode is competing to each other. The coupling of the wave to the plasma thermal energy via Landau resonance is brought up of the same order correction of ρ_i/a as the finite-gyroradius stabilization. Therefore, the two effects must be kept simultaneously. This fact implies the use of non-Maxwellian distribution function for improving the stability. For instance if one takes into account high energy ions, one can expect to enhance gyroradius stabilization much without increasing the coupling of the wave to the thermal energy of the plasma. The destabilization by the current can also be reduced. The

stability of the m=2 tearing mode in a high-β regime is because of the enhanced coupling to the drift branch and of the reduction of the electron drift u/v_i. If we consider an equilibrium where the longitudinal current is sustained by fast electrons, not by thermal electrons, then the excitation by the drift is reduced. This is because the radial region where the resonance takes place, $|k_\parallel \bar{V}_b| \simeq \omega_*$ ($\bar{V}_b$ being the fast electron velocity), is much localized to othe rational surface and the contribution to $\int \langle \tilde{J}_\parallel \tilde{E}_\parallel \rangle rdr$ is reduced. Therefore, by introducing new freedoms in equilibrium as a form of fast particles, we can divide the finite gyroradius effect and coupling to the plasma thermal energy and have possibility to reduce the instability growth rate. However, the non-Maxwellian distribution also affects the stability of other modes such as short wave length mode, one must perform a comprehensive analysis to find an optimum distribution function or even to know the advantage of new freedoms.

In formulating Eq. (6), we expand the perturbation distribution function with respect to ω_D/ω (ω_D being the curvature and ∇B drift frequency). This expansion is valid for the small ε, and even the MHD limit recovers the MHD analyses with reduced-set ordering. However, the Landau resonance is kept which is dominant resonance mechanism except for the flute mode. The compressional component of the magnetic field component $\tilde{B}_\zeta$ is neglected in Eq. (6) for the simplicity. This is consistent with the assumption that the magnetic well induced by the diamagnetic current is also neglected so long as one is concerned with the MHD driving force. The energy principle gives the δW associated with the ballooning mode as $\int -\vec{\xi} \cdot \nabla p \vec{\xi} \cdot \frac{1}{B^4}[\{\vec{B} \times \nabla(B^2+2p)\} \times \vec{B}]$ ($\vec{\xi}$ is the test displacement vector

in the energy principle), which shows that the ∇B caused by the plasma diamagnetic current cancels either for stabilizing or for destabilizing source. The $\tilde{B}_\zeta$ component on the other hand affects the resonant contribution. The term $|\phi_m + \frac{\omega}{k_\parallel c}\psi_m|^2$ in the integrand in the right-hand side of Eqs. (8) and (26) is replaced by $|\phi_m + \frac{\omega}{k_\parallel c}\psi_m + \frac{iv_i\tau\rho_i m}{ac}\tilde{B}_\zeta|^2$.[28] The correction by B_ζ is $O(\beta)$ and is small in the parameters treated in this article. The kinetic effects on the global modes are the very issues which require the analysis. For the study of the regime $\beta_p \sim R/a$, however, the much more accurate equilibrium (i.e., not expanded with respect to a/R) and the inclusion of the compressional component may be necessary. Further calculation with more accurate equilibrium must be performed to get a correct transition criterion between ES and MHD-like ballooning mode.

The stability diagram, summarized in Figure 2, shows that n=1 mode is almost always unstable in the current-carrying toroidal plasmas in the parameter range which is typical to tokamaks. However, the results show the existence of window for a good confinement. The Figure 10(b) illustrates the mode structure of kinetic ballooning mode. The electric perturbation is strongly peaked near $r=r_2$. When this mode becomes dominant instability and the perturbation grows up, the pressure profile around q=2 rational surface may become flat. Since the growth rate of this mode is proportional to ω_* at $r=r_2$, this flattening may easily prohibit the further growth of this mode before the central core plasma is seriously affected by this mode.[4-7] The window for a good global stability is surrounded by the boundaries, $q(0) > 1$ (for "m=1" mode stability), $\beta > \beta_c$ (for "m=2" tearing mode stability) and $\beta_p < \beta_{pc}$ (for MHD ballooning mode stability). We

see the importance of the plasma control to keep $q(0)$ greater than unity or to increase β-value before the q-value decreases by additional energy/momentum sources such as NBI or RF. To find the optimum path of the development of the plasma parameters, e.g. in the β-q space, we have to also investigate the high-n ballooning modes.

The stability criterion for the $m=2$ tearing mode, which is sensitive to the current density of electrons, differs from some previous works (say Ref.[14]). It should be emphasized that the "constant-ψ" approximation as well as the cut-off of the integral $\int^{x_c} \sigma dx$ (σ being the kinetic conductivity) at x_c is not correct. Even though the conductivity σ becomes small if x deviates much from the rational surface, it remains to be finite value[29] and the contribution to $\int_{x_c}^{x} \sigma dx$ at large value of $|x-x_c|$ can easily exceed the one from the vicinity of the rational surface.

The stability of the "m=2" tearing mode suggests that the occurrence of the major disruption becomes infrequent if the β-value becomes high enough. The optimistic view for the futrue high-β tokamak is expected. The critical-β value may be changed by the introduction of the trapped particles. The collision of transit electrons may not be neglected far from the center of the plasma column. Also important is the effect of the background fluctuations on the electron parallel conductivity. These problems remain to be for future analyses.

Acknowledgments

The authors would like to acknowledge Drs. T. Tsunematsu and M. Azumi and the members of the theory group of Japan Atomic Energy Research Institute as well as the members of the Institute for Fusion Studies (IFS) for valuable comments. Thanks are made to Dr. R. D. Hazeltine and Prof. H. L. Berk for elucidating discussions. Two of the authors (K. I. and S. I. I.) would like to acknowledge Prof. M. N. Rosenbluth for helpful discussions and hospitalities during their stay at IFS under the U.S./JAPAN Joint Institute for Fusion Theory, where this work is completed. Continuous encouragements by Prof. K. Nishikawa and Dr. T. Takeda are also appreciated.

References

1. V. D. Shafranov, Zh. Tekh., Fiz. 40 (1970) 241 [Sov. Phys. Tech. Phys. 15 (1970) 175] and J. Wesson, Nucl. Fusion 18 (1978) 87.

2. H.P. Furth, J. Killeen, and M. N. Rosenbluth, Phys. Fluids 6 (1963) 459.

3. B. Coppi, Phys. Fluids 7 (1964) 1501; 8 (1965) 2273.

4. G. Laval, R. Pellat and M. Vuillemin, in Plasma Physics and Controlled Nuclear Fusion Research (IAEA, Vienna, 1966) Vol. 2, p. 259.

5. M. Azumi, T. Tsunematsu, K. Itoh, T. Tuda, G. Kurita, T. Takeda, T. Takizuka, S. Tokuda, T. Matsuura, Y. Tanaka, S. Inoue, and M. Tanaka, in Plasma Physics and Controlled Nuclear Fusion Research (IAEA, Vienna, 1981) Vol. 1, p. 293.

6. K. Itoh, S.-I. Itoh, and T. Tuda, J. Phys. Soc. Japan 50 (1981) 655.

7. W. M. Tang, J. W. Connor and R. B. White, Nucl. Fusion 21 (1981) 891.

8. K. T. Tsang and D. J. Sigmar, Nucl. Fusion 21 (1981) 1227.

9. K. Itoh, S.-I. Itoh, S. Tokuda and T. Tuda, Nucl. Fusion 22 (1982) 1031.

10. G. Rewoldt, W. M. Tang and M. S. Chance, Phys. Fluids 25 (1982) 480.

11. D. Dobrott, D. B. Nelson, J. M. Greene, A. H. Glasser, M. S. Chance and E. A. Frieman, Phys. Rev. Lett. 39 (1977) 943.

12. J. W. Connor, R. J. Hastie and J. B. Taylor, Proc. Roy. Soc. A365 (1979) 1.

13. R. D. Hazeltine, D. Dobrott and T. S. Wang, Phys. Fluids 18 (1975) 1778.

14. J. F. Drake and Y. C. Lee, Phys. Fluids 20 (1977) 134.

15. M. N. Bussac, D. Edery, R. Pellat and J. L. Soule, Phys. Rev. Lett. 40 (1978) 500.

16. S.-I. Itoh and K. Itoh, Nucl. Fusion 21 (1981) 3.

17. K. Itoh and S.-I. Itoh, Phys. Lett. 82A (1981) 85.

18. M. N. Rosenbluth, R. Y. Dagazian and P. H. Rutherford, Phys. Fluids 16 (1973) 1894.

19. M. N. Bussac, R. Pellat, D. Edery and J. L. Soule, Phys. Rev. Lett. 35 (1975) 1638.

20. S. Tokuda, T. Tsunematsu, M. Azumi, T. Takizuka and T. Takeda, Nucl. Fusion 22 (1982) 661.

21. B. Coppi, R. Galvao, R. Pellat, M. N. Rosenbluth and P. H. Rutherford, Fiz. Plazmy 2 (1976) 961 [Sov. J. Plasma Phys. 2 (1976) 533].

22. M. Azumi, S. Tokuda, G. Kurita, T. Tsunematsu, T. Takizuka, T. Tuda, K. Itoh, Y. Tanaka and T. Takeda, JAERI-M Report 9787 (1981).

23. S. Yoshikawa, Phys. Fluids 17 (1974) 178.

24. K. Itoh, S.-I. Itoh, S. Tokuda and T. Tuda, HIFT-52 (Hiroshima, 1982).

25. T. Tuda, K. Itoh, S. Tokuda and S.-I. Itoh, Phys. Fluids 25 (1982) 1583.

26. S.-I. Itoh, K. Itoh and Y. Terashima, J. Phys. Soc. Japan 51 (1982) 983.

27. K. T. Tsang, J. C. Whitson and J. Smith, Phys. Fluids 22 (1980) 1689.

28. S. Inoue, K. Itoh and S. Yoshikawa, J. Phys. Soc. Japan 48 (1980) 973.

29. R. D. Hazeltine, private communication.

Figure Captions

Figure 1 -

Geometry and co-ordinates. x on R-axis denotes magnetic axis, which is shifted from center of magnetic surface of minor radius r by $|\Delta|$.

Figure 2 -

Stability and mode transition diagram on q_0-$\beta(0)$ plane. Solid line shows the boundary for the unstable mode and dashed line denotes the transition from MHD to kinetic mode. m=1 internal/tearing mode exists for $q(0) < 1 < q(a)$ and m=2 tearing mode is stabilized if $\beta(0) > 0.02$. Other parameters are: $R/a = 3$, $s = 2.25$, $q(a)/q(0) = 2.52$, $\rho_i/a = 1/200$, $\langle\beta\rangle \sim 0.4\beta(0)$, $T_e = T_i$, $M_i = 1836M_e$. n is always chosen to be unity.

Figure 3 -

Growth rate of the "m=1" mode (solid linie) as a function of β_p. $q(0) = 0.9$, $\rho_i/a = 1/200$ and s=3. Other parameters are standard. The dashed line shows the MHD limit ($\rho_i/a \to 0$, $E_\parallel \to 0$) showing $\gamma_{MHD} \to 0$ as $\beta_p \to 0$. The kinetic theory gives $\gamma > 0$ even if $\beta_p \to 0$.

Figure 4 -

ρ_i dependence of γ for $\beta_i = .001$, .003 and .005. γ/ω_A increases linearly as given by Eq. (17-2). $q(0) = 0.9$ and other parameters are standard.

Figure 5 -

Growth rate of the "m=1" mode (solid line) as a function of inverse aspect ratio. $q(0) = 0.9$, $\rho_i/a = 1/200$, $s=3$ and $\beta_p = 0.5$. Dashed line shows the MHD limit. Kinetic mode is unstable in the $a/R \to 0$ limit turning to be the tearing mode.

Figure 6 -

Growth rate vs. $q(0)$ for $\beta_i(0) = 0.005$, $\rho_i/a = 1/200$, $R/a = 3$ and $s=3$. The dashed line is the MHD limit of the toroidal mode ($\rho_i/a \to 0$, $\tilde{E}_\parallel \to 0$) - internal kink mode, while the dotted line is the cylindrical limit ($a/R \to 0$) - m=1 tearing mode. The transition between the kinetic tearing mode and the MHD mode is clearly shown.

Figure 7 -

Eigenmode structure for "m=1" mode for MHD unstable case (a) and MHD stable case (b). Solid line for real part and dashed line for imaginary part. Parameters are: $\rho_i/a = 1/100$, $R/a = 3$, $\beta_i(0) = .005$, $s = 2.25$, $q(0) = 0.9$ and $\omega/\omega_* = (-1.07, 2.40)$ for (a) and $\rho_i/a = 1/200$, $\beta_i(0) = .001$, $s=3$, $q(0) = 0.4$ and $\omega/\omega_* = (-0.1, 21.5)$ for (b). Other parameters are standard.

Figure 8 -

Growth rate for the n=1 ballooning mode normalized to ω_A. Dotted line shows γ/ω_*. Dashed line denotes the γ/ω_A in the MHD limit showing the critical β-value for instability. Below the critical condition, the instability turns to be kinetic one. $\rho_i/a - 1/200$, $q(0) = 1.7$ and other parameters are standard.

Figure 9 -

Eigenvalue for the ballooning mode for the MHD unstable case ($q(0) = 1.7$, solid line) and the growth rate for the MHD stable case ($q(0) = 1.2$, dashed line) vs. ρ_i/a. $\beta_i = 1/200$, $R/a = 3$ and other parameters are standard. Since β_i is kept constant the critical condition for MHD instability, $\beta_p > \beta_{pc}$, reduces to $q(0) \gtrsim 1.5$. For $\beta_p < \beta_{pc}$, $\gamma \to 0$ for $\rho_i/a \to 0$.

Figure 10 -

Eigenmode structure for the ballooning mode. (a) for the MHD unstable case ($\beta_i(0) = .005$) and (b) for the MHD stable case ($\beta_i(0) = .001$). Solid line for real part and dashed line for imaginary part. $\rho_i/a = 1/200$, $q(0) = 1.7$, $R/a = 3$, $s = 2.25$, and other parameters are standard. For the kinetic instability (b), the perturbation $\tilde{E}_\theta$ is strongly localized near the q=2 rational surface. The amplitude $|\tilde{B}_r|$ reduces and the mode finally becomes electrostatic mode for $\beta_i < M_e/M_i$.

Figure 11 -

Eigenmode structure of the "m=2" tearing mode for $\beta_i = 0.001$, $\rho_i/a = 1/200$, $q(0) = 0.9$, $s=3$, $R/a = 4$ and other parameters are standard. Solid lines for real part and dashed lines for imaginary part. The wave form of $\tilde{B}_{r2}$ shows the character of the m=2 tearing mode, and the parallel electric field exists in the region $|\omega_*/k_\parallel v_i| \gtrsim 1$. $\omega/\omega_* = (1.0, .02)$.

Figure 12 -

The growth rate of the m=2 tearing mode (solid line) as a function of β_i. $q(0) = 0.9$, $q(a) = 2.7$, $s=3$, $\rho_i/a = 1/1000$, $R/a = 4$ and other parameters are standard. The dashed line is $\gamma/|\omega_*|$ for the cylindrical limit. Toroidal effect further stabilizes the mode.

Figure 13 -

Stability criterion for the "m=2" tearing mode. $q(0) = 0.9$, $q(a) = 2.7$, $s=3$, $R/a = 4$ and other parameters are standard. The critical β value for stability is proportional to ρ_i/a.

Figure 14 -

Stability criterion for the "m=2" tearing mode (solid line). $\rho_i/a = 1/200$, $s=3$, $q(a)/q(0) = 3$, $R/a = 4$ and other parameters are standard. The instability region is localized to the low-β region for the toroidal plasma. Dashed line is for the cylindrical limit.

Figure 15 -

The eigenmode structure for the "m=2" tearing mode for stable case ($\beta_i = .01$). Other parameters are the same as Figure 11. The corrugation of the wave form shows the strong coupling to the drift branch, and the amplitudes of the m=1,3 comonents are enhanced. Solid line for real part and dashed line for imaginary part.

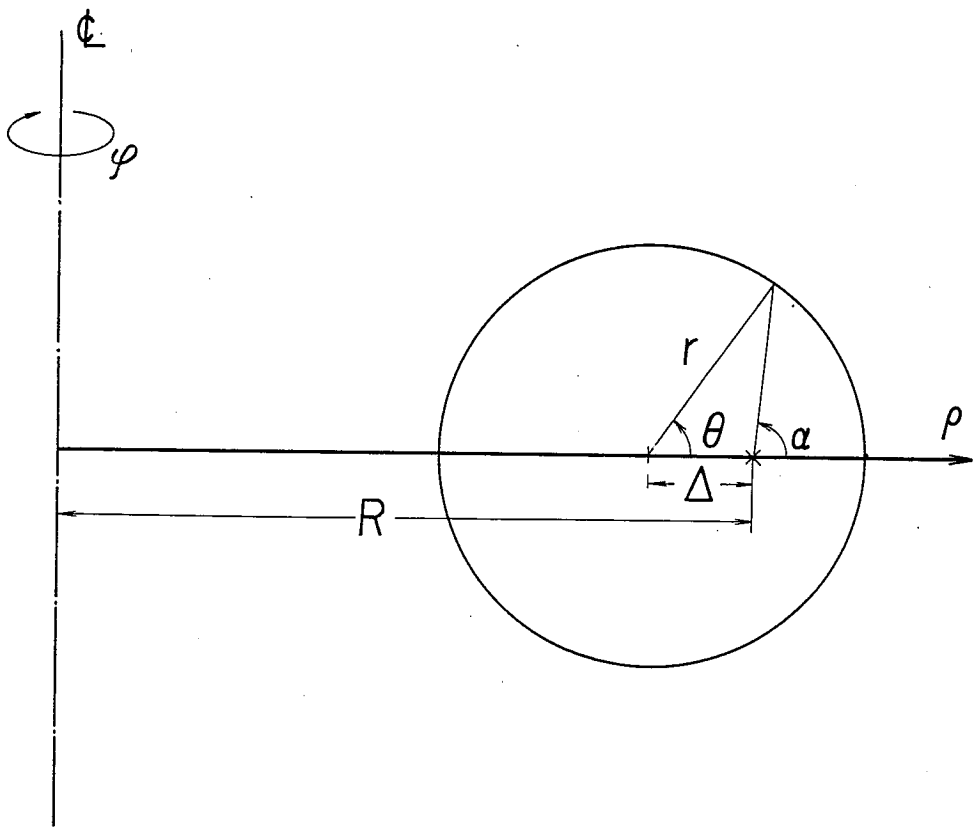

FIG.. 1

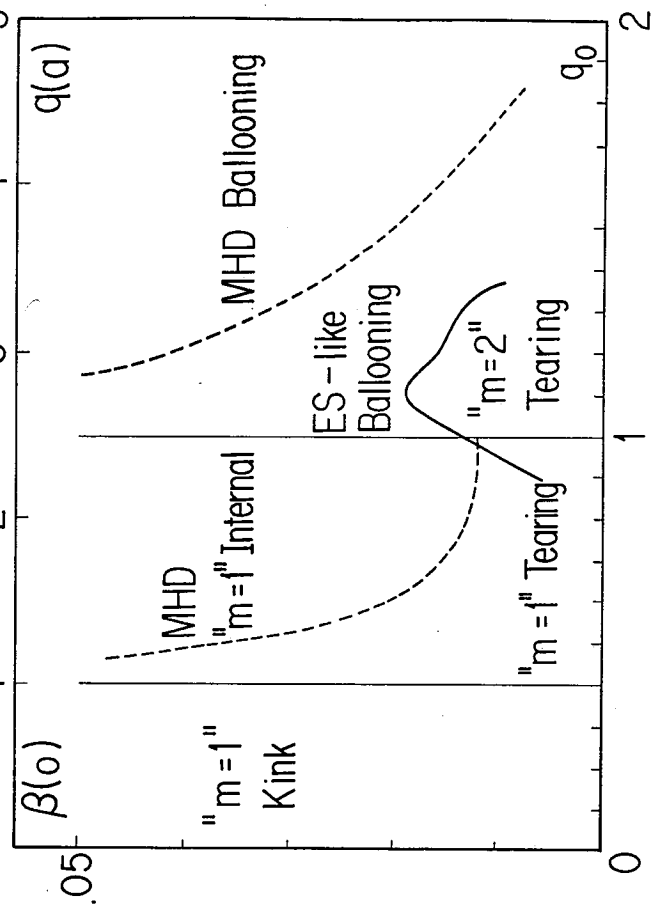
β(o)
q(a)
.05
0
1
2
3
4
5
1
2
q_o
"m=1" Kink
MHD "m=1" Internal
"m=1" Tearing
ES-like Ballooning
MHD Ballooning
"m=2" Tearing

FIG. 2

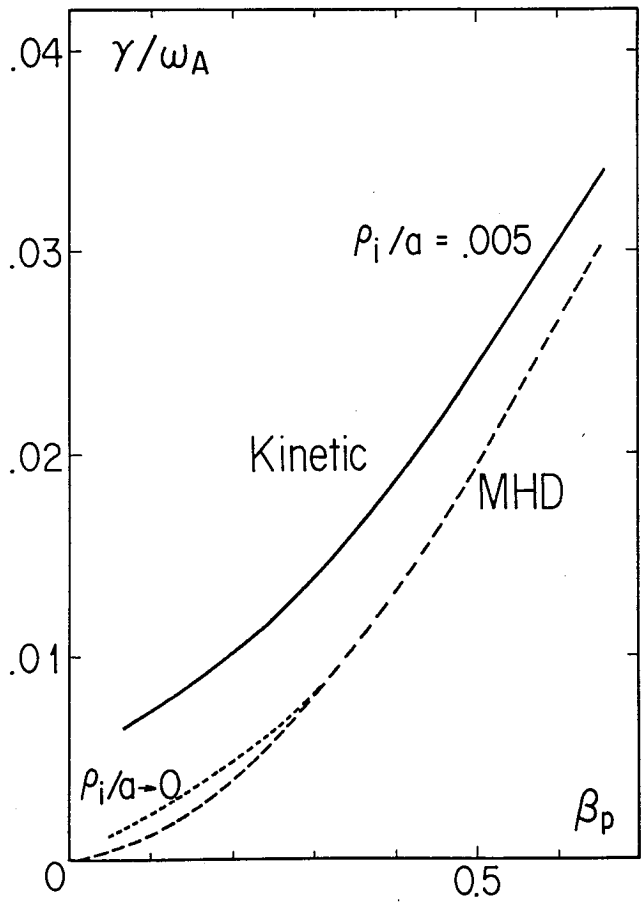
.04
γ/ω_A
.03
$\rho_i/a = .005$
.02
Kinetic
MHD
.01
$\rho_i/a \to 0$
β_p
0
0.5

FIG. 3

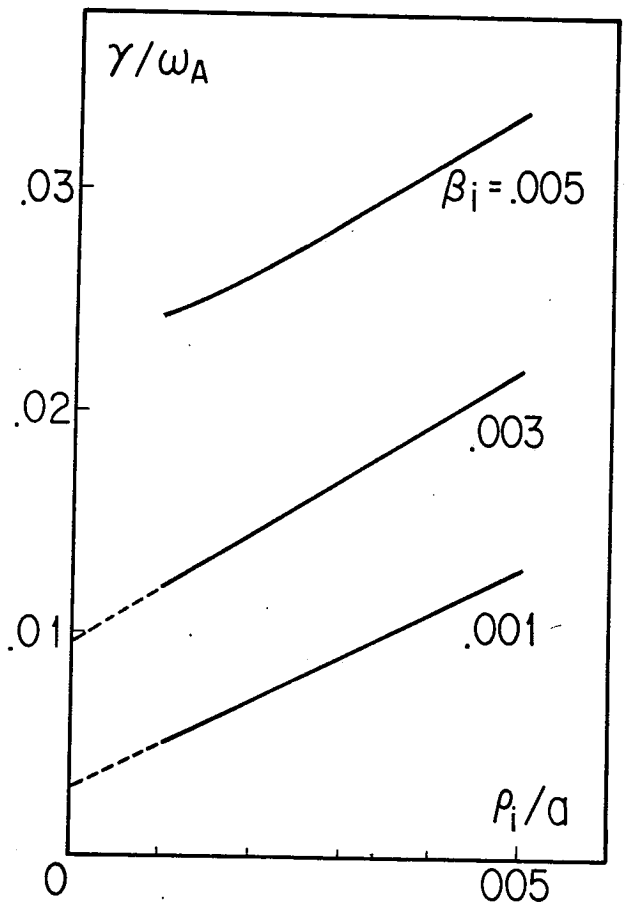

FIG. 4

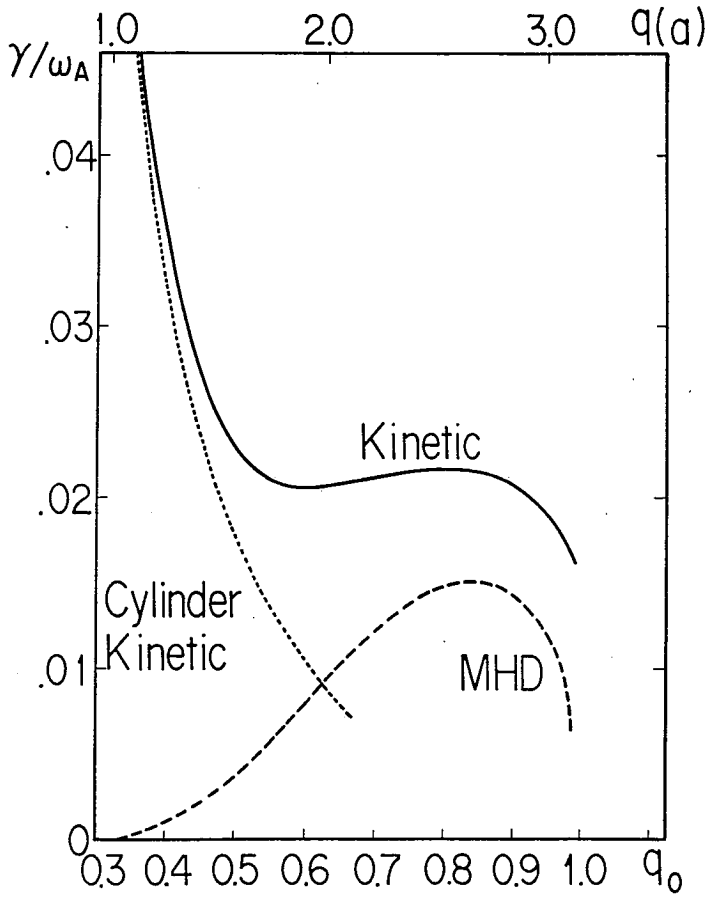
1.0
2.0
3.0
q(a)
γ/ω_A
.04
.03
.02
.01
0
Kinetic
Cylinder
Kinetic
MHD
0.3 0.4 0.5 0.6 0.7 0.8 0.9 1.0
q_0

FIG. 6

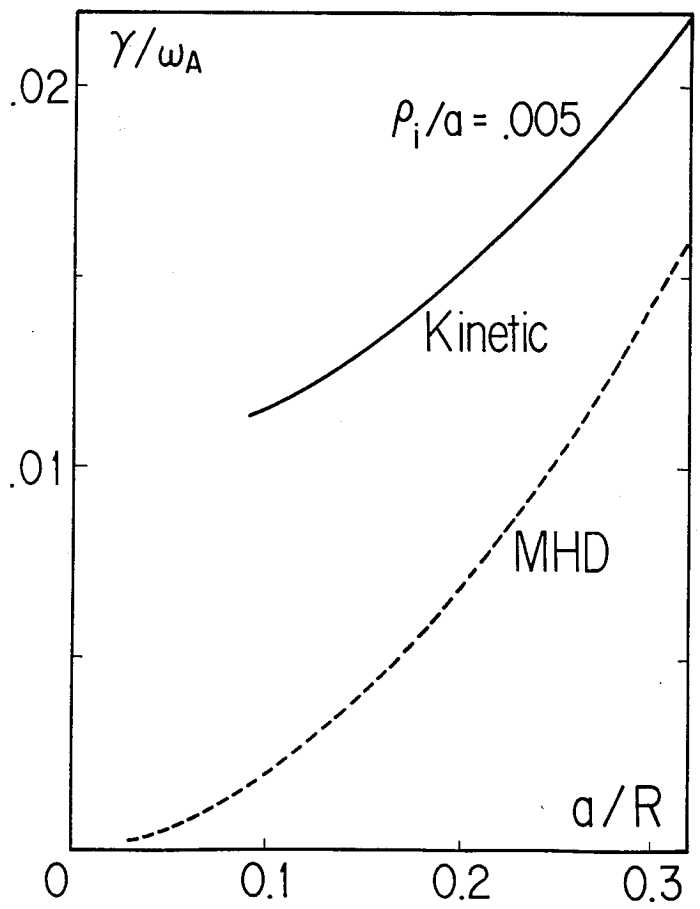

FIG. 5

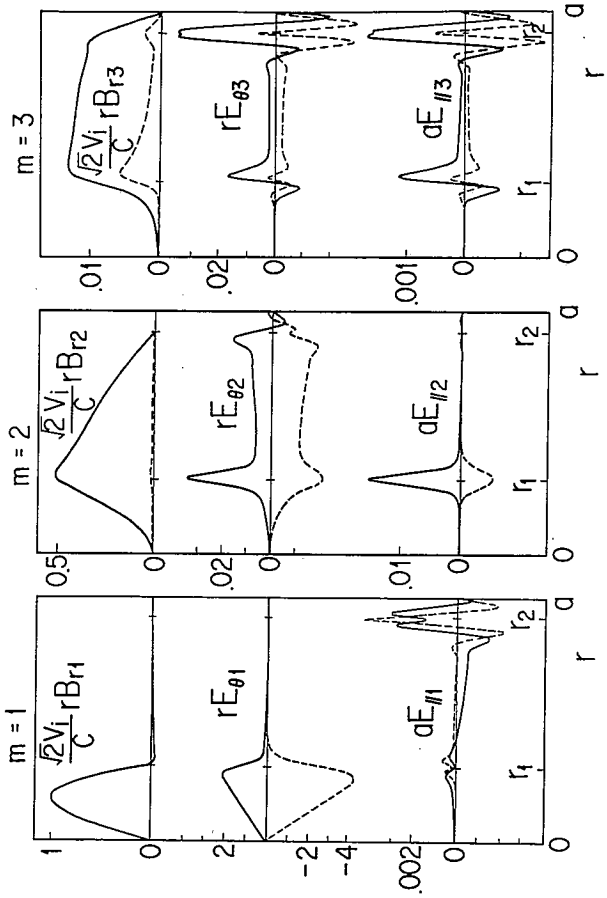
m = 1
m = 2
m = 3
$\frac{\sqrt{2}V_i}{C} rB_{r1}$
$rE_{\theta 1}$
$dE_{//1}$
$\frac{\sqrt{2}V_i}{C} rB_{r2}$
$rE_{\theta 2}$
$dE_{//2}$
$\frac{\sqrt{2}V_i}{C} rB_{r3}$
$rE_{\theta 3}$
$dE_{//3}$
r
a
r_1
r_2

FIG. 7a

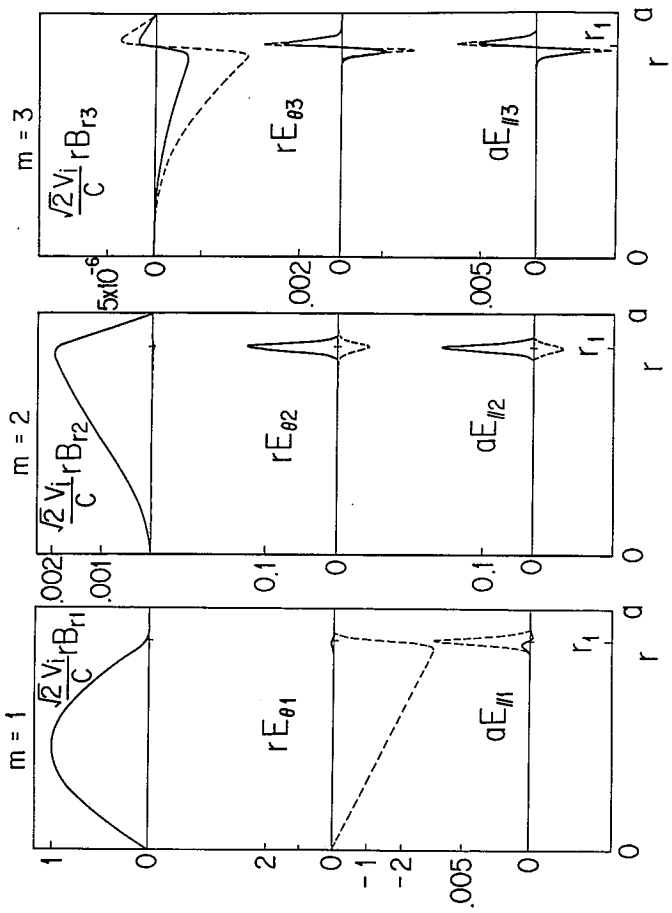
m = 1
m = 2
m = 3
$\frac{\sqrt{2}V_i}{c} rB_{r1}$
$\frac{\sqrt{2}V_i}{c} rB_{r2}$
$\frac{\sqrt{2}V_i}{c} rB_{r3}$
$rE_{\theta 1}$
$rE_{\theta 2}$
$rE_{\theta 3}$
$aE_{//1}$
$aE_{//2}$
$aE_{//3}$
1
0
2
0
-1
-2
.005
0
.002
.001
0.1
0
0.1
0
5x10^{-6}
0
.002
0
.005
0
r_1
r
a

FIG. 7b

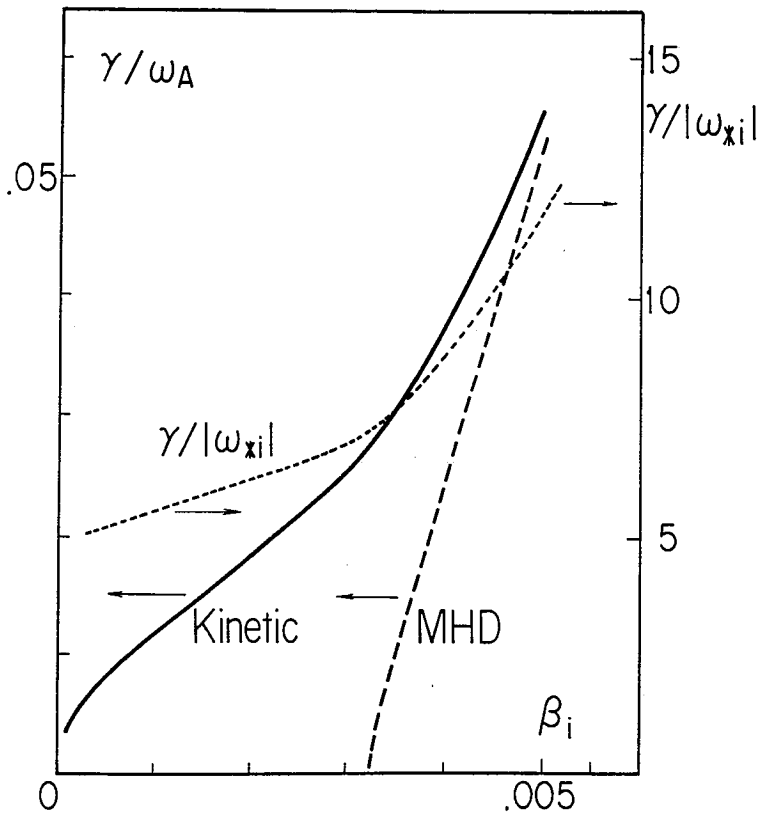

FIG. 8

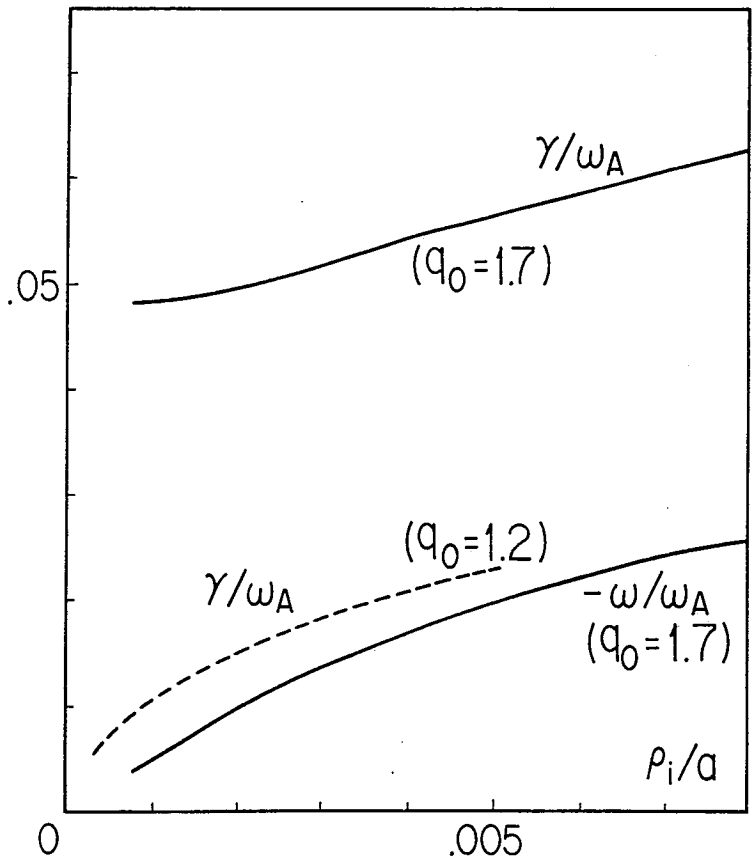
γ/ω_A
$(q_0=1.7)$
.05
$(q_0=1.2)$
γ/ω_A
$-\omega/\omega_A$
$(q_0=1.7)$
ρ_i/a
0
.005

FIG. 9

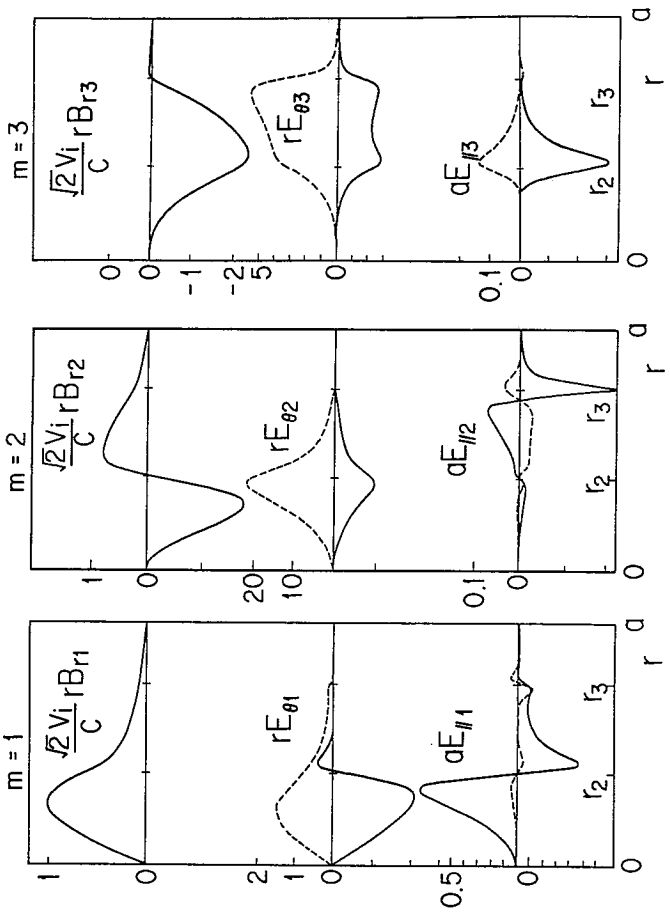
m = 1
m = 2
m = 3
$\frac{\sqrt{2}V_i}{c} rB_{r1}$
$\frac{\sqrt{2}V_i}{c} rB_{r2}$
$\frac{\sqrt{2}V_i}{c} rB_{r3}$
$rE_{\theta 1}$
$rE_{\theta 2}$
$rE_{\theta 3}$
$dE_{\parallel 1}$
$dE_{\parallel 2}$
$dE_{\parallel 3}$
r_2
r_3
r
a

FIG. 10a

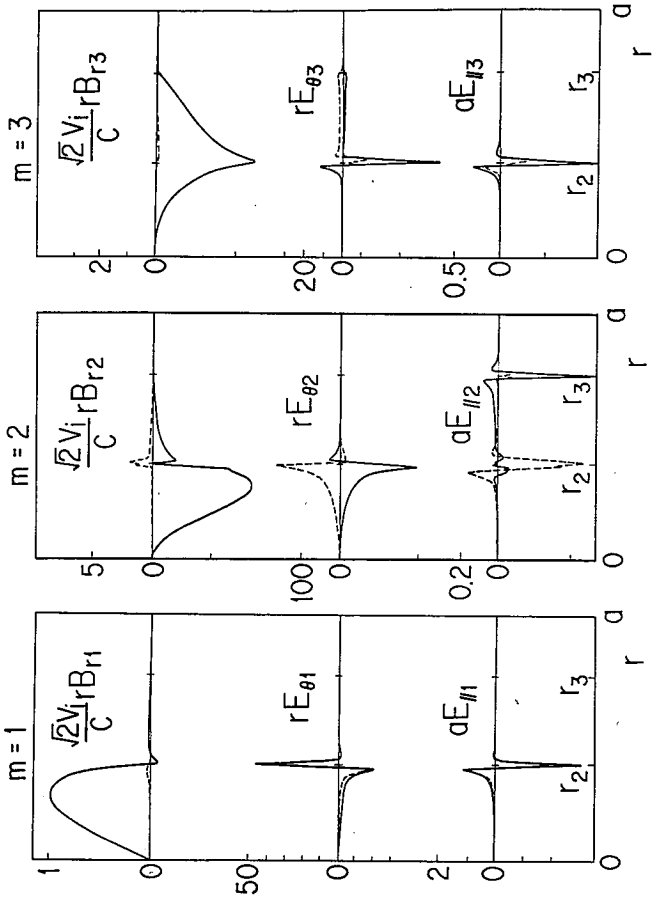
m = 1
m = 2
m = 3
$\frac{\sqrt{2}V_i}{c}rB_{r1}$
$\frac{\sqrt{2}V_i}{c}rB_{r2}$
$\frac{\sqrt{2}V_i}{c}rB_{r3}$
$rE_{\theta 1}$
$rE_{\theta 2}$
$rE_{\theta 3}$
$aE_{//1}$
$aE_{//2}$
$aE_{//3}$
r_2
r_3
r
a
1
0
50
2
5
100
0.2
20
0.5

FIG. 10b

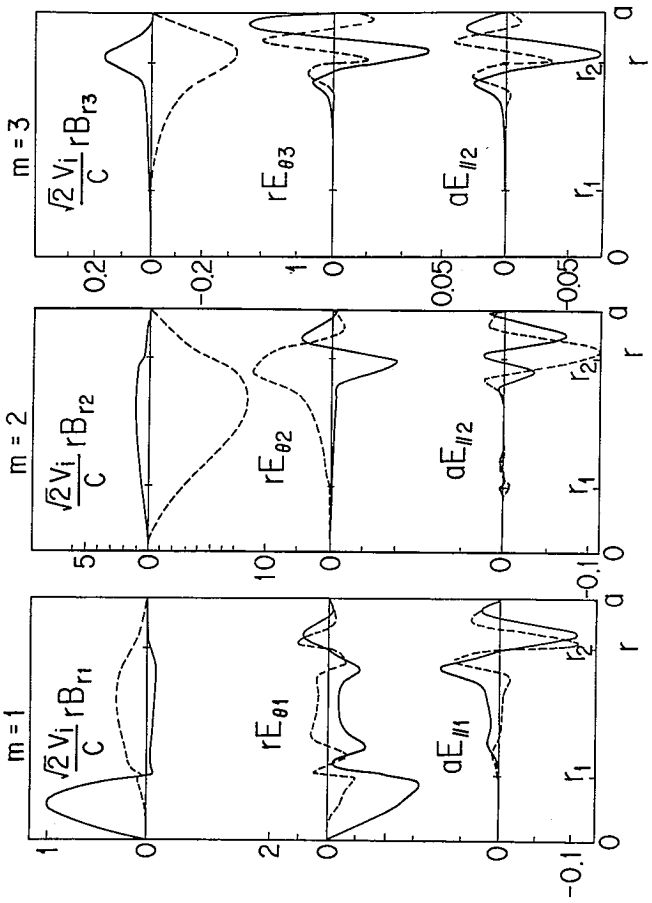
m = 1
m = 2
m = 3
$\frac{\sqrt{2}V_i}{c} rB_{r1}$
$\frac{\sqrt{2}V_i}{c} rB_{r2}$
$\frac{\sqrt{2}V_i}{c} rB_{r3}$
$rE_{\theta 1}$
$rE_{\theta 2}$
$rE_{\theta 3}$
$aE_{//1}$
$aE_{//2}$
$aE_{//2}$
r
a
r_1
r_2

FIG. 11

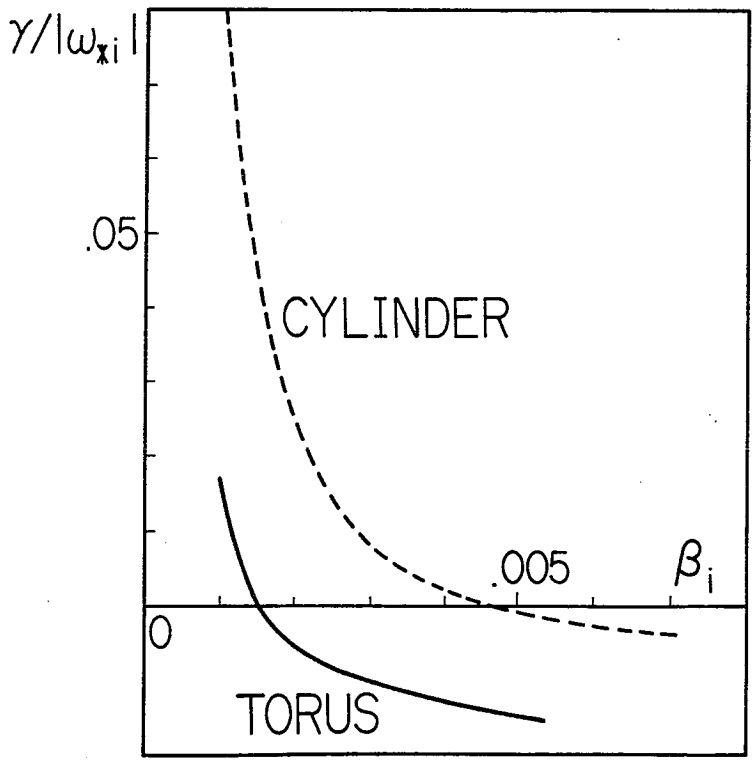

FIG. 12

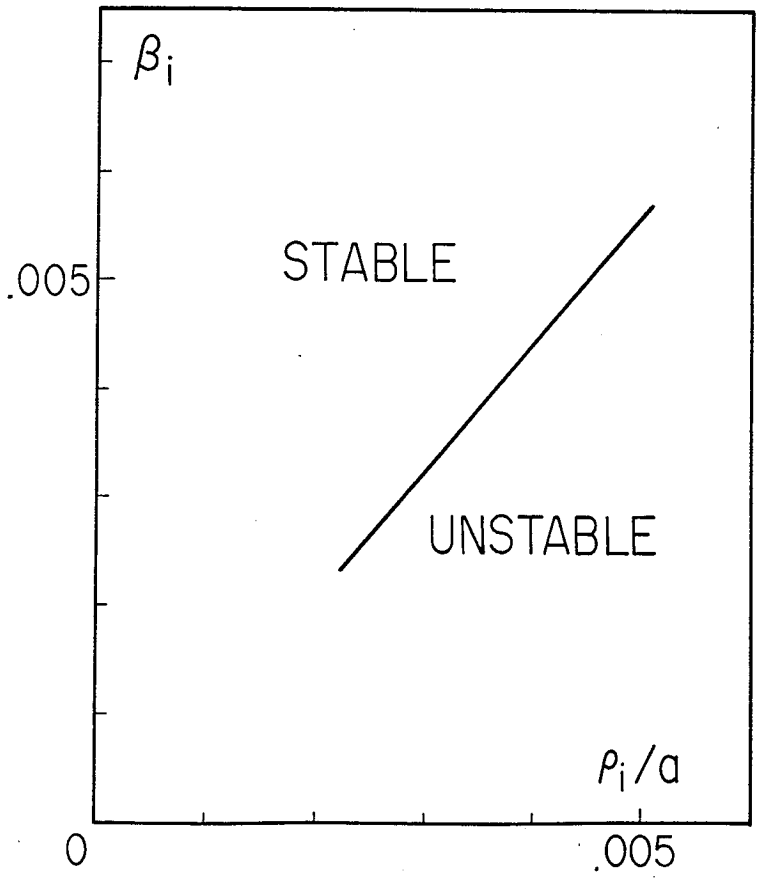

FIG. 13

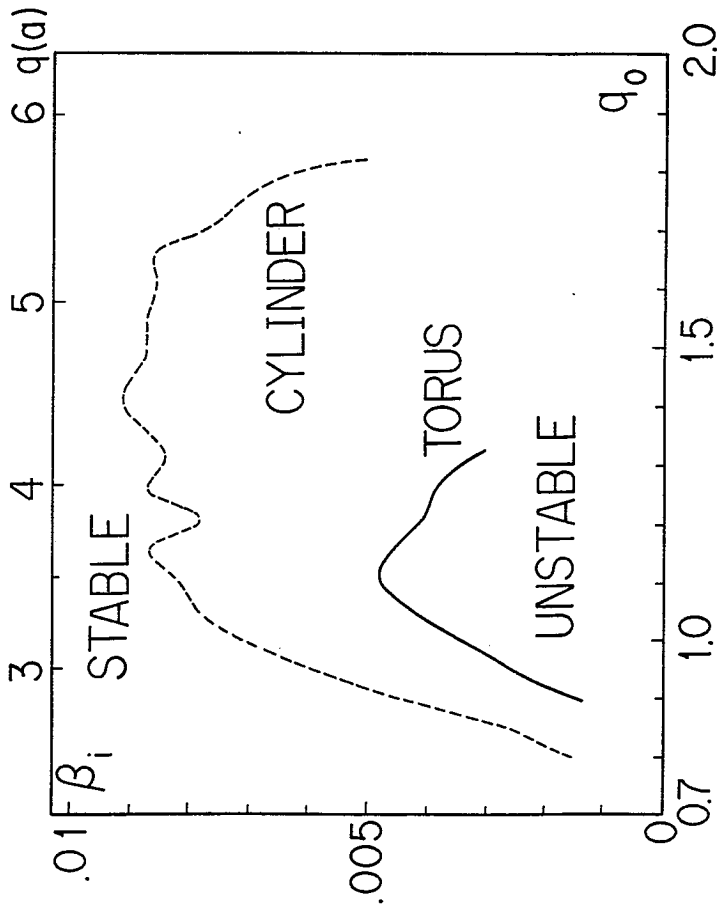
q(a)
6
5
4
3
β_i
.01
.005
0
0.7
1.0
1.5
2.0
q_o
STABLE
CYLINDER
TORUS
UNSTABLE

FIG. 14

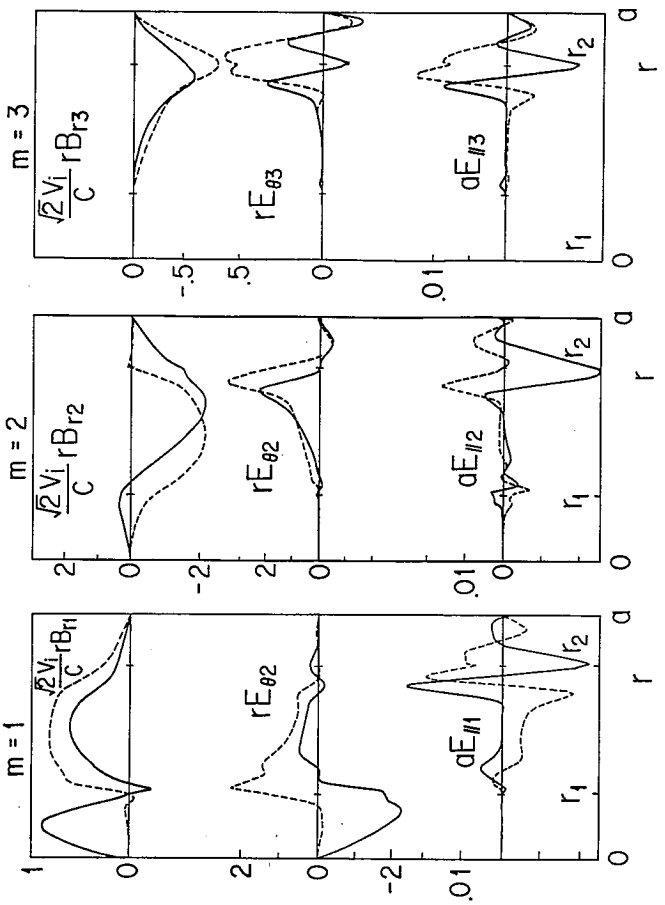
m = 1
m = 2
m = 3
$\frac{\sqrt{2}V_i}{c} rB_{r1}$
$\frac{\sqrt{2}V_i}{c} rB_{r2}$
$\frac{\sqrt{2}V_i}{c} rB_{r3}$
$rE_{\theta 2}$
$rE_{\theta 2}$
$rE_{\theta 3}$
$aE_{//1}$
$aE_{//2}$
$aE_{//3}$
r_1
r_2
r
a
1
0
2
-2
.01
-.5
.5

FIG. 15